

# 'À la Carte' Peptide Shuttles: Tools to Increase Their Passage across the Blood–Brain Barrier

Morteza Malakoutikhah,<sup>[a]</sup> Bernat Guixer,<sup>[a]</sup> Pol Arranz-Gibert,<sup>[a]</sup> Meritxell Teixidó,<sup>\*,[a]</sup> and Ernest Giralt<sup>\*,[a, b]</sup>

Noninvasive methods for efficient drug delivery to the brain is an unmet need. Molecular access to the brain is regulated by the blood–brain barrier (BBB) established by the endothelial cells of brain vessels. Passive diffusion is one of the main mechanisms that organic compounds use to travel through these endothelial cells. This passage across the BBB is determined mainly by certain physicochemical properties of the molecule such as lipophilicity, size, and the presence of hydrogen bond donors and acceptors. One emerging strategy to facilitate the passage of organic compounds across the BBB is the use of peptide shuttles.<sup>[1]</sup> In using this approach the permeability in front the BBB is, clearly, determined by the com-

bined physicochemical properties of both the cargo and the shuttle. Herein we report the synthesis of a series of variations of one of the more efficient peptide shuttles, (N-MePhe)<sub>n</sub>. These include diverse structural features such as various backbone stereochemistries or the presence of non-natural amino acids, including halogenated residues. In several cases, we assessed the BBB permeability of both the shuttles alone and linked to a few cargos. Our results show how factors such as stereochemistry or halogen content influences the passage across the BBB and, more importantly, opens the way to a strategy of peptide shuttles 'à la carte', in which a particular fine-tuned shuttle is used for each specific cargo.

## Introduction

Recent years have witnessed huge research efforts channeled into the discovery of new drugs and the development of strategies for their specific delivery. It is estimated that 1.5 billion people worldwide currently suffer from various central nervous system (CNS) disorders, and as the elderly population increases, these diseases will become a major health problem worldwide.<sup>[2,3]</sup> Most of the drugs currently on the market for CNS disorders are far from ideal because of their poor blood–brain barrier (BBB) penetration. More than 98% of small molecules do not cross the BBB, and the scenario is even worse for large-molecule drugs, including peptides, recombinant proteins, and monoclonal antibodies.<sup>[4]</sup> Transport across the BBB is one of the main challenges in the field of brain/CNS drug targeting using noninvasive methods.<sup>[5]</sup>

The BBB is the most important barrier protecting the CNS, although the blood–cerebrospinal fluid (CSF) interface plays a significant role in specific sites. The BBB is located in brain capillaries and is formed mainly by brain capillary endothelial

cells (which differ from those in peripheral tissues in that they have very few endocytotic vesicles and form tight junctions between them); however, pericytes, astrocytes, and neuronal cells also have key functions in the BBB.<sup>[6–9]</sup>

Despite the protective function of the BBB, it does not completely isolate the brain and the CNS, as it allows basic nutrients such as glucose, amino acids, ions, and gases such as O<sub>2</sub> and CO<sub>2</sub> to enter the brain. Influx mechanisms include the paracellular pathway (restricted because of tight junctions) and transcellular pathways, such as passive diffusion (normally limited to small and highly lipophilic molecules), carrier-mediated, receptor-mediated, and absorptive-mediated transport.<sup>[7,8]</sup>


BBB shuttles or Trojan-horse moieties (molecules with the capacity to enter the brain and carry a drug that is unable to cross the BBB unaided) are currently one of the most promising strategies to overcome the BBB.<sup>[1,3,10,11]</sup> In the case of passive diffusion, physicochemical properties entirely determine the capacity of molecules to cross biological membranes. Lipophilicity governed by the presence of polar groups and/or hydrogen bond donors/acceptors in the structure of a compound, molecular weight, peptide length, and amino acid sequence are considered the main determinants of the capacity of peptides to cross the BBB.<sup>[12]</sup>

After some years working with peptides that cross the BBB by passive diffusion and successfully using these molecules as BBB shuttles,<sup>[13–15]</sup> we envisaged other physicochemical features that may be relevant for this transport and that are usually overlooked. These properties, such as flexibility, halogenation, and stereochemistry, can be considered tools to increase and fine-tune the transport of compounds. In this regard, we se-

[a] Dr. M. Malakoutikhah,<sup>+</sup> B. Guixer,<sup>+</sup> P. Arranz-Gibert, Dr. M. Teixidó, Prof. E. Giralt  
Institute for Research in Biomedicine (IRB Barcelona)  
Baldiri Reixac 10, Barcelona, 08028 (Spain)  
E-mail: meritxell.teixido@irbbarcelona.org  
ernest.giralt@irbbarcelona.org

[b] Prof. E. Giralt  
Department of Organic Chemistry, University of Barcelona  
Martí i Franquès 1–11, Barcelona, 08028 (Spain)

[<sup>+</sup>] These authors contributed equally to this work.

 Supporting information for this article is available on the WWW under <http://dx.doi.org/10.1002/cmdc.201300575>.

lected a well-known family of shuttles that cross the BBB by passive diffusion<sup>[16]</sup> and studied the effect of factors such as halogen content and stereochemistry on their transport capacity.

## Results and Discussion

### Chirality

Cell membrane components such as phospholipids and proteins are chiral. Because all these components are commonly found enantiomerically pure in nature, it has been postulated<sup>[17]</sup> that stereoisomers could be discriminated in cell membranes. It was previously shown that biomembrane models such as micelles and vesicles can discriminate between homochiral and heterochiral enantiomers of dipeptides.<sup>[18–21]</sup> These studies hypothesized that in chiral aggregates recognition occurs in a chiral environment induced in an internal region of the aggregate by remote stereogenic centers. Therefore, chiral recognition cannot be simply ascribed to noncovalent-specific interactions between the solute and the monomers behaving as single entities, but is instead due to the aggregate as a whole. Therefore, potential discrimination can occur in regions of the aggregate/membrane that are quite far away from the stereogenic centers. In addition, these chiral interactions appear to confer a particular conformation to the enantiomers and diastereomers that finally determines the fate of the molecule when interacting with the membrane. Furthermore, another study demonstrated that diastereomeric peptides show distinctive lipophilicity and permeability across the BBB.<sup>[22]</sup>

To study the effect of peptide stereochemistry on membrane permeation, we prepared a library consisting of 16 stereoisomeric peptides (Table 1) and evaluated them by parallel artificial membrane permeability assay (PAMPA), which is the gold-standard method for assessing transport across the BBB via passive diffusion. All the peptides had four *N*-MePhe residues and were designed based on our previously reported peptide, Ac-(*N*-MePhe)<sub>4</sub>-CONH<sub>2</sub>, which showed high permeation in PAMPA studies.<sup>[13,14]</sup> HPLC retention time in reversed-phase columns (HPLC *t<sub>R</sub>*) is a good measure of the polarity of a molecule, especially when comparing stereoisomers of the same compound.<sup>[23,24]</sup> We used these retention times to rank our molecules in terms of lipophilicity. We found that the homochiral peptides (LLLL and DDDD), although less lipophilic than the rest of the heterochiral peptides, exhibited higher permeability and lower membrane retention (%*R*) in PAMPA (Table 1). Between the two homochiral versions, the all-D version showed higher permeation than the previously reported all-L version.

One could expect that in passive diffusion, the greater the lipophilicity, the greater the permeability across membranes. However, for these 16 peptides, an inverse correlation was detected between lipophilicity and permeability ( $r=0.757$ , Figure 1a). Furthermore, permeability correlated inversely with membrane retention (%*R*;  $r=0.888$ , Figure 1b). In contrast,

**Table 1.** Effective permeability ( $P_e$ ), percentage of transport ( $T_{4h}$ ), and membrane retention (*R*) in the PAMPA after 4 h and HPLC *t<sub>R</sub>* of 16 stereoisomers and control compounds, propranolol and carbamazepine.<sup>[a]</sup>

Compound <sup>[b]</sup>	$P_e$ [ $\times 10^6$ cm s <sup>-1</sup> ] <sup>[c]</sup>	$T_{4h}$ [%]	<i>R</i> [%]	HPLC <i>t<sub>R</sub></i> [min]
propranolol	5.7 ± 0.9	10.7 ± 1.4	55.1 ± 9.7	4.96
carbamazepine	8.5 ± 0.3	15.1 ± 0.4	< 1	6.60
Ac-(DDDD)-CONH <sub>2</sub>	9.4 ± 0.9	16.4 ± 1.3	20.7 ± 5.0	3.8
Ac-(LLLL)-CONH <sub>2</sub>	6.6 ± 0.3	12.2 ± 0.5	42 ± 0.2	4
Ac-(LLLD)-CONH <sub>2</sub>	5.6 ± 0.2	10.5 ± 0.4	48.4 ± 0.5	4.2
Ac-(DDDL)-CONH <sub>2</sub>	6.1 ± 0.1	11.4 ± 0.1	45.4 ± 0.7	4.3
Ac-(LDDD)-CONH <sub>2</sub>	4 ± 0.9	7.8 ± 1.6	76 ± 2.5	4.3
Ac-(DLLL)-CONH <sub>2</sub>	4 ± 1.1	7.7 ± 1.9	58.1 ± 7.5	4.3
Ac-(DLDD)-CONH <sub>2</sub>	3.1 ± 0.1	6.2 ± 0.1	64.1 ± 0.4	4.5
Ac-(LDDL)-CONH <sub>2</sub>	4.4 ± 1.4	8.4 ± 2.5	43.3 ± 4.1	4.5
Ac-(DDLl)-CONH <sub>2</sub>	2.9 ± 0.4	5.9 ± 0.8	74.2 ± 6.2	4.7
Ac-(LLDD)-CONH <sub>2</sub>	2.3 ± 0.1	4.6 ± 0.2	81.6 ± 1.5	4.8
Ac-(LLDL)-CONH <sub>2</sub>	4.1 ± 0.2	8.0 ± 0.4	64.4 ± 0.8	4.9
Ac-(DDLd)-CONH <sub>2</sub>	2.7 ± 0.3	5.4 ± 0.7	75.1 ± 3.6	5
Ac-(DLDD)-CONH <sub>2</sub>	3.3 ± 0.1	6.6 ± 0.2	65.7 ± 0.6	5.2
Ac-(LDLL)-CONH <sub>2</sub>	5 ± 0.4	9.6 ± 0.7	56.7 ± 2.3	5.2
Ac-(LDLD)-CONH <sub>2</sub>	3 ± 0.2	6.0 ± 0.4	71.3 ± 0.1	5.3
Ac-(DLdL)-CONH <sub>2</sub>	2 ± 0.2	4.2 ± 0.4	78.4 ± 1.8	5.3

[a] Data are expressed as the mean ± SD of  $n=3$  experiments performed in triplicate.

[b] D and L stand for D-*N*-MePhe and L-*N*-MePhe respectively. [c] Low permeability:  $P_e < 0.1 \times 10^{-6}$  cm; medium permeability:  $0.1 \times 10^{-6}$  cm  $< P_e < 1 \times 10^{-6}$  cm; high permeability:  $P_e > 1 \times 10^{-6}$  cm.

there was a direct correlation between lipophilicity and membrane retention (%*R*;  $r=0.723$ , Figure 1c). These results indicate that in this series of stereoisomeric peptides, homochiral peptides (LLLL and DDDD) had the optimal lipophilicity. The heterochiral peptides might show excessive lipophilicity, hampering their passage across the PAMPA membrane due to excessive retention within the membrane. The observed behavior is probably a consequence of differences in the more stable conformations adopted by each stereoisomer in the presence of the lipid bilayers. Our findings are consistent with previous studies reporting that heterochiral dipeptides (LD and DL) bond more strongly to chiral micellar phases (being trapped in the hydrophobic micellar portion of the described model) than homochiral enantiomers (LL and DD).<sup>[18–20]</sup> Looking now to the presence or absence of enantiomeric discrimination along all the stereoisomers,<sup>[19,20,25]</sup> our observations in the PAMPA membrane showed that enantiomeric discrimination was remarkable for most of the enantiomeric pairs (although it was very low for the pairs LDDD/DLLL and DDDL/LLLD). Although there is not a clear global trend, in general the observed enantiomeric discrimination is higher for heterochiral enantiomers than for homochiral peptides.

### À la carte peptide length

It is clear from our previous work that there is a relationship between PAMPA permeability and the number of *N*-MePhe residues in a BBB shuttle peptide.<sup>[13,14]</sup> In a series of *N*-MePhe oligomers (Ac-(*N*-MePhe)<sub>*n*</sub>-CONH<sub>2</sub>  $n=2-10$ ), an increase in peptide chain length enhanced PAMPA permeability up to the peptide with four *N*-MePhe residues, namely Ac-(*N*-MePhe)<sub>4</sub>-CONH<sub>2</sub>.

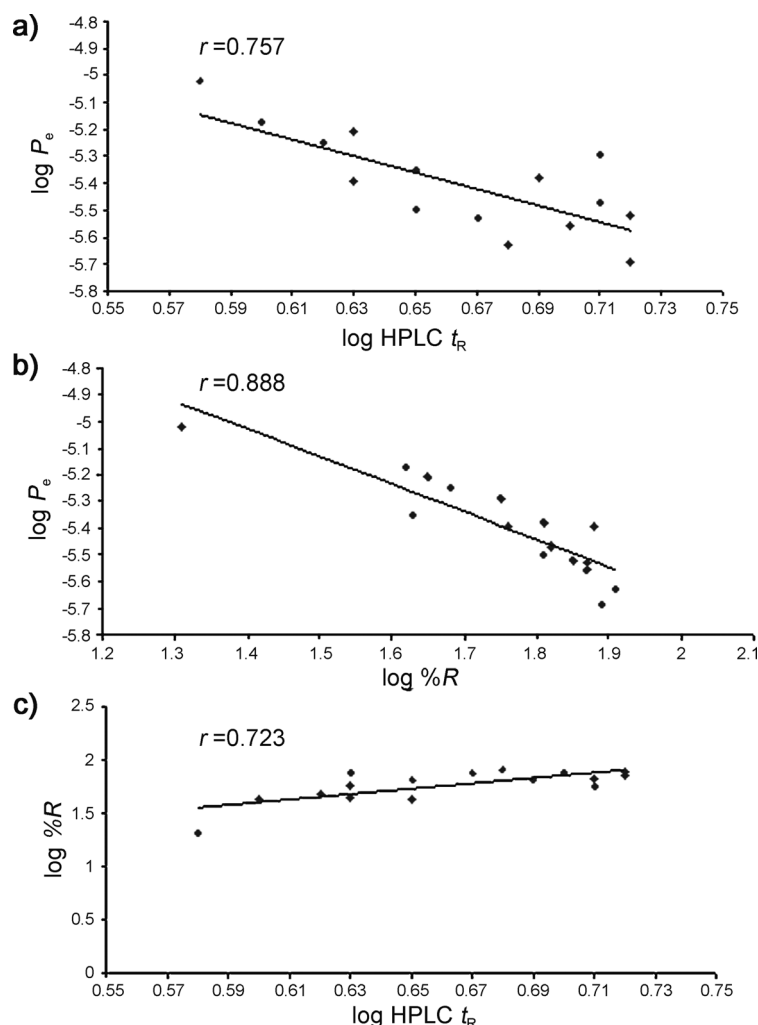


**Figure 1.** a) Inverse correlation between  $\log P_e$  of 16 stereoisomers and their  $\log \text{HPLC } t_R$ . b) Inverse correlation between  $\log P_e$  of 16 stereoisomers and their  $\log \%R$ . c) Correlation between  $\log \text{HPLC } t_R$  of 16 stereoisomers and their  $\log \%R$ .

However, when the peptide had more than four residues, permeability dropped considerably. In this regard, we explored whether  $\text{H}-(\text{N-MePhe})_3\text{-CONH}_2$  and  $\text{H}-(\text{N-MePhe})_2\text{-CONH}_2$ , when coupled to a neurodrug cargo (L-DOPA, GABA, and NIP), show better performance as carriers than the original tetrapeptides. The results are summarized in Table 2.

#### Case 1, L-DOPA: 3,4-dihydroxy-L-phenylalanine

L-DOPA is a prodrug of dopamine that has been used for the last four decades to treat Parkin-

son's disease. Dopamine cannot enter the brain unaided; however, L-DOPA crosses the BBB by means of a large natural amino acid carrier. Once inside the brain, L-DOPA is enzymatically converted into dopamine by aromatic L-amino acid decarboxylase. However, L-DOPA administration is hindered by several side effects caused by dopamine formation in the periphery.<sup>[26–28]</sup> L-DOPA derivatization through an amide bond has been reported to inhibit the decarboxylation reaction in the periphery and to enhance L-DOPA in the brain.<sup>[29–31]</sup> Furthermore, because L-DOPA competes with other L-amino acids to gain access to the brain, it would be desirable to deliver this drug to this organ by a noncompetitive passive transport mechanism.

L-DOPA is unable to cross the PAMPA membrane unaided. In contrast, our peptide BBB shuttles transported this drug across the membrane and showed medium to high permeability. The tetrapeptide showed the highest PAMPA permeability (measured as  $P_e$  or percent transport after 4 h) and lipophilicity (measured by IAMC as  $k_{\text{IAM}}$ ) (Table 2). However, the dipeptide with the lowest lipophilicity presented slightly better PAMPA permeability than the tripeptide. In Case 1, the longest shuttle exhibits the best transport capacity.

#### Case 2, GABA: 4-aminobutyric acid

A decreased concentration of GABA, the dominant inhibitory neurotransmitter in the CNS, is associated with several brain diseases. Increasing the concentration of this amino acid in the CNS may serve to treat these brain disorders; however, GABA permeation across the BBB is insufficient to enhance its levels in the brain.<sup>[32–35]</sup> Some GABA derivatives show higher permeation across the BBB than GABA alone.<sup>[36–38]</sup>

**Table 2.** Effective permeability ( $P_e$ ), percentage of transport ( $T_{4h}$ ) in the PAMPA, and lipophilicity ( $k_{\text{IAM}}$ ) of X-(N-MePhe)<sub>n</sub>-CONH<sub>2</sub> (X = L-DOPA, GABA, and NIP;  $n = 2–4$ ) and control compounds (propranolol, carbamazepine) after 4 h.<sup>[a,b]</sup>

Compound	$P_e$ [ $\times 10^6 \text{ cm s}^{-1}$ ]	$T_{4h}$ [%]	$k_{\text{IAM}}$
propranolol	$6.6 \pm 0.4$	$12.2 \pm 0.6$	1.9
carbamazepine	$8.5 \pm 0.3$	$15.1 \pm 0.4$	2.1
L-DOPA-N-MePhe-N-MePhe-CONH <sub>2</sub>	$0.6 \pm 0.03$	$1.2 \pm 0.05$	$2.4 \pm 0.1$
L-DOPA-N-MePhe-N-MePhe-N-MePhe-CONH <sub>2</sub>	$0.4 \pm 0.03$	$0.9 \pm 0.07$	$9.7 \pm 0.4$
L-DOPA-N-MePhe-N-MePhe-N-MePhe-N-MePhe-CONH <sub>2</sub>	$1.1 \pm 0.1$	$2.4 \pm 0.2$	$29.6 \pm 1.3$
GABA-N-MePhe-N-MePhe-CONH <sub>2</sub>	$0.2 \pm 0.02$	$0.5 \pm 0.04$	$1.7 \pm 0.05$
GABA-N-MePhe-N-MePhe-N-MePhe-CONH <sub>2</sub>	$0.3 \pm 0.01$	$0.6 \pm 0.03$	$7.2 \pm 0.1$
GABA-N-MePhe-N-MePhe-N-MePhe-N-MePhe-CONH <sub>2</sub>	$0.4 \pm 0.06$	$0.8 \pm 0.1$	$12.5 \pm 2.2$
NIP-N-MePhe-N-MePhe-CONH <sub>2</sub>	$0.9 \pm 0.1$	$1.9 \pm 0.3$	$1.6 \pm 0.01$
NIP-N-MePhe-N-MePhe-N-MePhe-CONH <sub>2</sub>	$1.5 \pm 0.2$	$3.1 \pm 0.3$	$9.6 \pm 0.01$
NIP-N-MePhe-N-MePhe-N-MePhe-N-MePhe-CONH <sub>2</sub>	$1.4 \pm 0.1$	$2.8 \pm 0.2$	$8.1 \pm 1.3$

[a] Data are expressed as the mean  $\pm$  SD of  $n = 3$  experiments performed in triplicate. [b] Reported by our research group in 2008 and 2010.<sup>[13,14]</sup> Only results of tetrapeptides (X-N-MePhe-N-MePhe-N-MePhe-CONH<sub>2</sub>, X = N-MePhe, Cha, 1-Nal) were already reported.

To test the potential of our peptides as carriers of GABA, this drug was attached to the peptides in solid phase. Peptides showed a small difference in PAMPA permeability, whereas distinctive capacity factors were detected in IAMC (Table 2). In Case 2, transport is less dependent on length, although again, the tetrapeptide shuttle is more efficient.

### Case 3, NIP: nipecotic acid

The level of GABA in the brain can also be increased by using either GABA inhibitors, which prevent this unusual amino acid from being used by neurons and glial cells, or GABA receptor agonists. Nipecotic acid fulfills these two requirements; however, its inability to gain access to the brain limits its application for the treatment of diseases affecting this organ.<sup>[34,39,40]</sup>

As third cargo, we conjugated NIP to the peptides and assessed the transport of the resulting constructs in PAMPA and IAMC (Table 2). Here the tripeptide showed higher PAMPA permeability than the dipeptide and the tetrapeptide. In summary, we found here a first example of the 'à la carte' concept; that is, there is an optimal length for the (N-MePhe)<sub>n</sub> shuttle, but for each cargo this length can be different ( $n=4$  for L-DOPA and GABA;  $n=3$  for NIP).

### Incorporation of non-natural amino acids

Chemical diversity of peptides can be widely expanded by incorporation of non-natural amino acids carrying a variety of special side chains. To explore the use of non-natural amino acids as tools to modulate BBB transport we first explored the use of two non-halogenated Phe analogues, cyclohexylalanine (Cha) and 2-naphthylalanine (2NaI), as N-terminal residues in our peptide BBB shuttles.

Hence the three neurodrug cargos (L-DOPA, GABA, and NIP) were attached to Cha- and 2NaI-containing peptides of variable length, and the behavior in PAMPA and IAMC assays was studied (Table 3). For L-DOPA, the dipeptides probably have the optimum lipophilicity required to penetrate the PAMPA phospholipids, with dipeptide Cha-N-MePhe-CONH<sub>2</sub> displaying the greatest capacity to carry this drug through the PAMPA membrane. For GABA, Cha and 2NaI tripeptides showed the best performance as shuttles and greatly improved their

**Table 3.** Effective permeability ( $P_e$ ) and percentage of transport ( $T_{4h}$ ) in the PAMPA after 4 h and lipophilicity ( $k_{IAM}$ ) of X-Y-(N-MePhe)<sub>n</sub>-CONH<sub>2</sub> (X = L-DOPA, GABA, and NIP; Y = N-MePhe, Cha, and 2NaI;  $n=1-3$ ) and control compounds (propranolol and carbamazepine).<sup>[a,b]</sup>

Compound	$P_e$ [ $\times 10^6$ cm s <sup>-1</sup> ]	$T_{4h}$ [%]	$k_{IAM}$
propranolol	6.2 ± 0.6	11.5 ± 1.1	1.9
carbamazepine	9.3 ± 0.8	16.2 ± 1.1	2.1
L-DOPA-N-MePhe-N-MePhe-CONH <sub>2</sub>	0.6 ± 0.03	1.2 ± 0.05	2.4 ± 0.1
L-DOPA-Cha-N-MePhe-CONH <sub>2</sub>	2.2 ± 0.1	4.4 ± 0.2	24.7 ± 1
L-DOPA-2NaI-N-MePhe-CONH <sub>2</sub>	1.8 ± 0.1	3.6 ± 0.2	32.6 ± 1.8
L-DOPA-N-MePhe-N-MePhe-N-MePhe-CONH <sub>2</sub>	0.4 ± 0.03	0.9 ± 0.07	9.7 ± 0.4
L-DOPA-Cha-N-MePhe-N-MePhe-CONH <sub>2</sub>	1.7 ± 0.2	3.5 ± 0.4	60.1 ± 1.6
L-DOPA-2NaI-N-MePhe-N-MePhe-CONH <sub>2</sub>	1 ± 0.03	2 ± 0.1	68.4 ± 2.7
L-DOPA-N-MePhe-N-MePhe-N-MePhe-N-MePhe-CONH <sub>2</sub>	1.1 ± 0.1	2.4 ± 0.2	29.6 ± 1.3
L-DOPA-Cha-N-MePhe-N-MePhe-N-MePhe-CONH <sub>2</sub>	0.7 ± 0.06	1.4 ± 0.1	> 128 <sup>[c]</sup>
L-DOPA-2NaI-N-MePhe-N-MePhe-N-MePhe-CONH <sub>2</sub>	0.3 ± 0.1	0.7 ± 0.2	102 ± 6.2
GABA-N-MePhe-N-MePhe-CONH <sub>2</sub>	0.2 ± 0.02	0.5 ± 0.04	1.7 ± 0.05
GABA-Cha-N-MePhe-CONH <sub>2</sub>	1.4 ± 0.05	2.8 ± 0.1	10.6 ± 0.1
GABA-2NaI-N-MePhe-CONH <sub>2</sub>	1.2 ± 0.1	2.5 ± 0.4	13.7 ± 0.03
GABA-N-MePhe-N-MePhe-N-MePhe-CONH <sub>2</sub>	0.3 ± 0.01	0.6 ± 0.03	7.2 ± 0.1
GABA-Cha-N-MePhe-N-MePhe-CONH <sub>2</sub>	2.3 ± 0.4	4.6 ± 1.4	13 ± 0.04
GABA-2NaI-N-MePhe-N-MePhe-CONH <sub>2</sub>	1.5 ± 0.4	3 ± 0.7	22.9 ± 0.4
GABA-N-MePhe-N-MePhe-N-MePhe-N-MePhe-CONH <sub>2</sub>	0.4 ± 0.06	0.8 ± 0.1	12.5 ± 2.2
GABA-Cha-N-MePhe-N-MePhe-N-MePhe-CONH <sub>2</sub>	0.4 ± 0.1	0.8 ± 0.3	28.2 ± 6.7
GABA-2NaI-N-MePhe-N-MePhe-N-MePhe-CONH <sub>2</sub>	0.2 ± 0.02	0.4 ± 0.04	30.2 ± 4.4
NIP-N-MePhe-N-MePhe-CONH <sub>2</sub>	0.9 ± 0.1	1.9 ± 0.3	1.6 ± 0.01
NIP-Cha-N-MePhe-CONH <sub>2</sub>	3.2 ± 0.2	6.3 ± 0.3	10.1 ± 0.1
NIP-2NaI-N-MePhe-CONH <sub>2</sub>	2.2 ± 0.1	4.4 ± 0.3	14.1 ± 0.02
NIP-N-MePhe-N-MePhe-N-MePhe-CONH <sub>2</sub>	1.5 ± 0.2	3.1 ± 0.3	9.6 ± 0.01
NIP-Cha-N-MePhe-N-MePhe-CONH <sub>2</sub>	1.8 ± 0.06	3.7 ± 0.07	20.4 ± 0.7
NIP-2NaI-N-MePhe-N-MePhe-CONH <sub>2</sub>	1.5 ± 0.04	3.1 ± 0.08	33.9 ± 0.3
NIP-N-MePhe-N-MePhe-N-MePhe-N-MePhe-CONH <sub>2</sub>	1.4 ± 0.1	2.8 ± 0.2	8.1 ± 1.3
NIP-Cha-N-MePhe-N-MePhe-N-MePhe-CONH <sub>2</sub>	1.2 ± 0.1	2.5 ± 0.2	> 128 <sup>[b]</sup>
NIP-2NaI-N-MePhe-N-MePhe-N-MePhe-CONH <sub>2</sub>	1.1 ± 0.06	2.4 ± 0.1	30.4 ± 1.5

[a] Data are expressed as the mean ± SD of  $n=3$  experiments performed in triplicate. [b] Reported by our research group in 2008 and 2010.<sup>[13,14]</sup> Only results of tetrapeptides (X-N-MePhe-N-MePhe-N-MePhe-CONH<sub>2</sub>, X = N-MePhe, Cha, 1-Nal) were already reported. [c] Retention time > 60 min in the IAMC HPLC column.

PAMPA permeability compared with tetrapeptides. The tripeptide Cha-(N-MePhe)<sub>2</sub>-CONH<sub>2</sub> showed the best shuttling performance for GABA. In the case of nipecotic acid, we observed that the N-MePhe tetrapeptide coupled to NIP exhibited better PAMPA permeability than tetrapeptides with Cha and 2NaI. Dipeptides enhanced NIP transport considerably for this cargo, especially in the case of Cha-N-MePhe-CONH<sub>2</sub>, which showed a greater capacity to transfer this neurodrug than the other peptides.

Finally, we decided to explore the effect of halogenation as a way to modulate peptide shuttle lipophilicity and consequently their capacity to cross the BBB.<sup>[41-45]</sup> For this purpose we studied the effect of chlorination of the phenylalanine residue on the dipeptide (H-N-MePhe-N-MePhe-CONH<sub>2</sub>) and tripeptide (H-N-MePhe-N-MePhe-N-MePhe-CONH<sub>2</sub>) neurodrug shuttle conjugates. On the one hand, we synthesized (*p*-Cl)-N-MePhe analogues of those constructs. N-Methylation of residues substituted on their aromatic rings such as Tyr, 3-pyridylalanine (3-Pal), and (*p*-Cl)Phe is not trivial.<sup>[46]</sup> However, we used a protocol (see Supporting Information) that allows N-methylation of (*p*-Cl)Phe in solid phase with great purity and without the formation of byproducts. On the other hand, we prepared the corresponding non-N-methylated chlorinated compounds, namely H-(*p*-Cl)Phe-N-MePhe-CONH<sub>2</sub> and H-(*p*-Cl)Phe-(*p*-Cl)Phe-

**Table 4.** Effective permeability ( $P_e$ ), percentage of transport ( $T_{4h}$ ), membrane retention ( $R$ ) in the PAMPA after 4 h, and lipophilicity ( $k_{IAM}$ ) of X-(Y)<sub>n</sub>-N-MePhe-CONH<sub>2</sub> (X = L-DOPA, GABA, and NIP; Y = N-MePhe, (p-Cl)N-MePhe and [(p-Cl)Phe]; n = 1–2) and control compounds (propranolol, carbamazepine).<sup>[a]</sup>

Compound	$P_e$ [ $\times 10^6$ cm s <sup>-1</sup> ]	$T_{4h}$ [%]	$R$ [%]	$k_{IAM}$
propranolol	6.2 ± 0.6	11.5 ± 1.1	33.3 ± 4	1.9
carbamazepine	9.3 ± 0.8	16.2 ± 1.1	< 1	2.1
L-DOPA-N-MePhe-N-MePhe-CONH <sub>2</sub>	0.6 ± 0.03	1.2 ± 0.05	< 1	2.4 ± 0.1
L-DOPA-(p-Cl)N-MePhe-N-MePhe-CONH <sub>2</sub>	1.9 ± 0.1	3.9 ± 0.2	5.1 ± 0.4	7.2 ± 0.1
L-DOPA-(p-Cl)Phe-N-MePhe-CONH <sub>2</sub>	1.6 ± 0.01	3.3 ± 0.02	12.7 ± 1.1	16.1 ± 0.4
L-DOPA-N-MePhe-N-MePhe-N-MePhe-CONH <sub>2</sub>	0.4 ± 0.03	0.9 ± 0.07	29.8 ± 3.4	9.7 ± 0.4
L-DOPA-(p-Cl)N-MePhe-(p-Cl)N-MePhe-N-MePhe-CONH <sub>2</sub>	1.5 ± 0.1	3 ± 0.2	25.5 ± 5.2	67 ± 1
L-DOPA-(p-Cl)Phe-(p-Cl)Phe-N-MePhe-CONH <sub>2</sub>	0.4 ± 0.03	0.8 ± 0.07	86.8 ± 2.4	> 128 <sup>[b]</sup>
GABA-N-MePhe-N-MePhe-CONH <sub>2</sub>	0.2 ± 0.02	0.5 ± 0.04	< 1	1.7 ± 0.05
GABA-(p-Cl)N-MePhe-N-MePhe-CONH <sub>2</sub>	0.7 ± 0.1	1.5 ± 0.2	6.5 ± 2.4	6.2 ± 0.1
GABA-(p-Cl)Phe-N-MePhe-CONH <sub>2</sub>	1.8 ± 0.3	3.7 ± 0.6	15.3 ± 3	7.1 ± 0.1
GABA-N-MePhe-N-MePhe-N-MePhe-CONH <sub>2</sub>	0.3 ± 0.01	0.6 ± 0.03	< 1	7.2 ± 0.1
GABA-(p-Cl)N-MePhe-(p-Cl)N-MePhe-N-MePhe-CONH <sub>2</sub>	1.7 ± 0.03	3.5 ± 0.05	20.3 ± 3.4	53.5 ± 1.1
GABA-(p-Cl)Phe-(p-Cl)Phe-N-MePhe-CONH <sub>2</sub>	1.6 ± 0.1	3.2 ± 0.3	35.8 ± 0.2	96.3 ± 3.3
NIP-N-MePhe-N-MePhe-CONH <sub>2</sub>	0.9 ± 0.1	1.9 ± 0.3	< 1	1.6 ± 0.01
NIP-(p-Cl)N-MePhe-N-MePhe-CONH <sub>2</sub>	1.5 ± 0.03	3.1 ± 0.05	< 1	5.7 ± 0.1
NIP-(p-Cl)Phe-N-MePhe-CONH <sub>2</sub>	1.7 ± 0.1	3.5 ± 0.5	7.6 ± 2.1	7.2 ± 0.1
NIP-N-MePhe-N-MePhe-N-MePhe-CONH <sub>2</sub>	1.5 ± 0.2	3.1 ± 0.3	< 1	9.6 ± 0.01
NIP-(p-Cl)N-MePhe-(p-Cl)N-MePhe-N-MePhe-CONH <sub>2</sub>	3.1 ± 0.2	6.2 ± 0.3	12.1 ± 0.9	56.2 ± 1.4
NIP-(p-Cl)Phe-(p-Cl)Phe-N-MePhe-CONH <sub>2</sub>	2 ± 0.3	4.1 ± 0.6	28.5 ± 0.6	103.7 ± 1.4

[a] Data are expressed as the mean ± SD of n = 3 experiments performed in triplicate. [b] Retention time > 60 min in the IAMC HPLC column.

N-MePhe-CONH<sub>2</sub>, in order to compare the respective influence of N-methylation and chlorination on lipophilicity and PAMPA permeability.

As expected, chlorination increased the lipophilicity of all the analogues tested with all cargos relative to the parent compounds (Table 4). Data also suggest differences in the lipophilicity of chlorinated peptides [H-(p-Cl)Phe-N-MePhe-CONH<sub>2</sub> or H-(p-Cl)Phe-(p-Cl)Phe-N-MePhe-CONH<sub>2</sub>] and chlorinated-N-methylated peptides [H-(p-Cl)N-MePhe-N-MePhe-CONH<sub>2</sub> or H-(p-Cl)N-MePhe-(p-Cl)N-MePhe-N-MePhe-CONH<sub>2</sub>], with the (p-Cl)Phe analogue, unexpectedly, being more lipophilic than the (p-Cl)N-MePhe one. In addition, we observed that the peptide with chlorinated Phe was more lipophilic than that with N-methylated Phe. Moreover, the addition of two chlorine atoms (Table 4) gave rise to a greater difference between the lipophilicity of chlorinated-N-methylated peptide and N-methylated peptide [H-(p-Cl)N-MePhe-(p-Cl)N-MePhe-N-MePhe-CONH<sub>2</sub> vs. H-N-MePhe-N-MePhe-N-MePhe-CONH<sub>2</sub>], beyond that of the addition of a single chlorine [H-(p-Cl)N-MePhe-N-MePhe-CONH<sub>2</sub> vs. H-N-MePhe-N-MePhe-CONH<sub>2</sub>].

We found that chlorination significantly increased the efficiency of peptide passage across the PAMPA phospholipids. For the dipeptides, when GABA and NIP were used as cargos, chlorinated peptide exhibited greater transport than the N-methylated and chlorinated-N-methylated peptides. These results indicate that while N-methylation of Phe enhanced PAMPA permeability relative to Phe, N-methylation of (p-Cl)Phe decreased peptide transport through the PAMPA membrane, probably due to the impact of N-methylation on the peptide conformation in a way that decreases the interaction between peptide and membrane and consequently decreases both lipophilicity and permeability.<sup>[47]</sup> However, in the case of L-DOPA, chlorinat-

ed-N-methylated peptide was the most permeating analogue, while it was less lipophilic than the chlorinated peptide alone. For all three cargos, the peptide with chlorinated Phe showed greater PAMPA permeability than that with N-methylated Phe.

For the tripeptide, with all cargos chlorinated peptide with higher lipophilicity showed less PAMPA permeability than chlorinated-N-methylated peptide. This greater lipophilicity may cause retention of the peptide in the membrane, as observed in PAMPA experiments (Table 4). Plotting lipophilicity versus PAMPA permeability provided correlations of  $r = 0.998$ ,  $r = 0.933$ , and  $r = 0.836$  for NIP, GABA, and L-DOPA dipeptides, respectively. However, for the tripeptides, a good correlation between lipophilicity and PAMPA permeability was not found except for GABA ( $r = 0.971$ ). These findings suggest that in order to obtain the greatest permeability, either chlorination or chlorination-N-methylation should be applied, 'à la carte' depending on the peptide sequence, as tools to fine-tune shuttle transport capacity.

## Conclusions

We have introduced the concept of 'à la carte' BBB peptide shuttles, which could prompt those in the field to abandon the search for a universal shuttle and, instead, to evolve an optimal shuttle for each cargo by fine-tuning structural features such as peptide length and halogen content. This concept could likely find application in other areas of drug delivery related to passage through other biological barriers, such as oral or transdermal drug delivery. We also observed that BBB permeability is not severely hampered (and can even be enhanced) when modifying the configuration of backbone stereogenic centers. This observation opens the way to the future



use of D-amino acid containing BBB shuttles in order to improve their 'in vivo' stability in the presence of proteases.

## Experimental Section

### Materials and methods

Protected amino acids and resins were supplied by Luxembourg Industries (Tel-Aviv, Israel), Neosystem (Strasbourg, France), Calbiochem-Novabiochem AG (Laüfelfingen, Switzerland), Bachem AG (Bubendorf, Switzerland), or Iris Biotech (Marktredwitz, Germany). PyBOP was supplied by Calbiochem-Novabiochem AG. DIEA, ninhydrin, and  $\beta$ -mercaptoethanol were obtained from Fluka Chemika (Buchs, Switzerland). HOAt was purchased from GL Biochem Shanghai Ltd. (Shanghai, China). Solvents for peptide synthesis and RP-HPLC were obtained from Scharlau or SDS (Barcelona, Spain). Trifluoroacetic acid was purchased from KaliChemie (Bad Wimpfen, Germany). Other chemicals used were purchased from Aldrich (Milwaukee, WI, USA) and were of the highest purity commercially available. PAMPA plates and PAMPA system solution were from pLON (Woburn, MA, USA). Porcine polar brain lipid extract (PBLEP) was purchased from Avantis Polar Lipids (Alabaster, AL, USA). IAMC column (10 $\times$ 4.6 mm, 12  $\mu$ m, 300 Å, IAM.PC.DD2 column) was from Regis Technologies Inc. (Morton Grove, IL, USA). Mass spectra were recorded on a MALDI Voyager DE RP time-of-flight (TOF) spectrometer (PE Biosystems, Foster City, CA, USA) using an ACH matrix. High-resolution mass spectra were recorded on an LTQ-FT Ultra (Thermo Scientific). HPLC chromatograms were recorded on a Waters model Alliance 2695 with photodiode array detector 996 from Waters (Waters, Milford, MA, USA) using a Symmetry C<sub>18</sub> column (150 $\times$ 4.6 mm $\times$ 5  $\mu$ m, 100 Å, Waters), solvents: H<sub>2</sub>O (0.045% TFA) and MeCN (0.036% TFA), flow: 1 mL min<sup>-1</sup> and Millennium software version 4.0. HPLC-MS [Waters model Alliance 2796, quaternary pump, UV/Vis dual absorbance detector Waters 2487, ESI-MS model Micromass ZQ and Masslynx version 4.0 software (Waters)] was done using a Symmetry 300 C<sub>18</sub> column (150 $\times$ 3.9 mm $\times$ 5  $\mu$ m, 300 Å, Waters), solvents: H<sub>2</sub>O (0.1% formic acid) and MeCN (0.07% formic acid), flow: 1 mL min<sup>-1</sup>. The products were purified in a Waters 600 with dual absorbance detector (Waters 2487), and a Symmetry C<sub>18</sub> column (100 $\times$ 30 mm $\times$ 5  $\mu$ m, 100 Å, Waters), solvents H<sub>2</sub>O (0.1% TFA) and MeCN (0.05% TFA), flow: 10 mL min<sup>-1</sup>.

### General protocols for solid-phase synthesis

Syntheses were performed on a 100- $\mu$ mol scale each; in all cases L-amino acids were used. Solid-phase peptide elongation and other solid-phase manipulations were done manually in polypropylene syringes, each fitted with a polyethylene porous disk. Solvents and soluble reagents were removed by suction. Washings between synthetic steps were done with DMF (5 $\times$ 30 s) and CH<sub>2</sub>Cl<sub>2</sub> (5 $\times$ 30 s) using 5 mL solvent per gram of resin each time. During couplings the mixture was allowed to react with intermittent manual stirring.

**Identification tests:** The Kaiser colorimetric assay<sup>[48]</sup> was used for the detection of solid-phase bound primary amines, while the De Clercq test<sup>[49]</sup> was used for secondary amines bound to the solid phase.

**Initial conditioning of resin:** The Sieber resin<sup>[50]</sup> was conditioned by washing with CH<sub>2</sub>Cl<sub>2</sub> (5 $\times$ 30 s) and DMF (5 $\times$ 30 s) followed by a 20% piperidine solution in DMF (2 $\times$ 1 min and 1 $\times$ 10 min) to remove the Fmoc group. Finally, the resin was washed with DMF (5 $\times$ 30 s).

**Fmoc group removal:** The Fmoc group was removed by treating the resin with 20% piperidine in DMF (3–4 mL (g resin)<sup>-1</sup>, 2 $\times$ 1 min and 1 $\times$ 10 min). To remove the Fmoc group from Fmoc-N-MePhe-OH and Fmoc-Pro-OH, an additional treatment with DBU, toluene, piperidine, DMF (5:5:20:70; 1 $\times$ 5 min) was performed.

### Coupling methods

**Method 1, coupling of the first amino acid onto the Sieber resin:** N-Protected N-methylated phenylalanine (4 equiv, 160.5 mg), PyBOP (4 equiv, 208 mg), and HOAt (12 equiv, 163.3 mg) were added sequentially to the resin in DMF (3 mL) followed by DIEA (12 equiv, 204  $\mu$ L). The mixture was allowed to react with intermittent manual stirring for 1.5 h. The solvent was removed by filtration; the resin was washed with DMF (5 $\times$ 30 s) and CH<sub>2</sub>Cl<sub>2</sub> (5 $\times$ 30 s). The extent of coupling was monitored by the Kaiser colorimetric assay.

**Method 2, coupling of second amino acid and the following amino acid onto the Sieber resin:** The procedure was the same as for the first, except that N-protected phenylalanine was used. The coupling was repeated two more times, and the extent of coupling was checked by the De Clercq test.

### Amino acid N-alkylation

The N-methylation of phenylalanine was performed by using the method described by Miller and Scanlan.<sup>[51]</sup> This process can be divided into three steps: A) protection and activation with *o*-nitrobenzenesulfonyl chloride (*o*-NBS), B) deprotonation and methylation, and C) *o*-NBS removal.

**A) Protection and activation with *o*-NBS:** To perform the protection, *o*-NBS (3 equiv, 67 mg) and collidine (5 equiv, 66  $\mu$ L) in CH<sub>2</sub>Cl<sub>2</sub> were added to the resin. The reaction was left with intermittent manual stirring for 1 h, and this step was repeated once and checked by the Kaiser test.

**B) Deprotonation and methylation:** Methyl *p*-nitrobenzenesulfonate (4 equiv, 86.9 mg) and MTBD (3 equiv, 43  $\mu$ L) in DMF were added to the resin and left for 30 min, and this step was repeated once.

**C) *o*-NBS removal:** To remove *o*-NBS,  $\beta$ -mercaptoethanol (10 equiv, 70  $\mu$ L) and DBU (5 equiv, 75  $\mu$ L) in DMF were added to the resin, and the mixture was left to react for 10 min under a nitrogen atmosphere. This process was repeated once for 40 min.

### Levodopa coupling

Amine-protected levodopa (4 equiv, 168 mg), PyBOP (4 equiv, 218 mg), and HOAt (12 equiv, 163.3 mg) were sequentially added to the resin in DMF (3 mL) followed by DIEA (12 equiv, 204  $\mu$ L). The mixture was allowed to react with intermittent manual stirring for 1.5 h. The solvent was removed by filtration, and the resin was washed with DMF (5 $\times$ 30 s) and CH<sub>2</sub>Cl<sub>2</sub> (5 $\times$ 30 s). The coupling was repeated two more times in the case of coupling on N-MePhe. The extent of coupling was checked by the De Clercq test or the Kaiser colorimetric assay.

### GABA/Nip coupling

The procedure was the same as for levodopa, except that Fmoc-GABA-OH or Fmoc-Nip-OH was used.

### Cleavage of the peptides

Final amide peptides were cleaved from the resin using 2% TFA in  $\text{CH}_2\text{Cl}_2$  (6 × 3 min).

### Product workup and RP-HPLC purification

After cleavage of the peptides, the solvent was evaporated by  $\text{N}_2$ . The residue was dissolved in  $\text{H}_2\text{O}/\text{MeCN}$  (1:1) and then lyophilized. The peptides were purified by reversed-phase (RP)-HPLC using a symmetry  $\text{C}_{18}$  column (100 × 30 mm × 5  $\mu\text{m}$ , 100 Å, Waters), at a 10  $\text{mL min}^{-1}$  flow rate with the following solvents: A,  $\text{H}_2\text{O}$  with 0.1% TFA; B, MeCN with 0.05% TFA.

### Product characterization

The identity of the compounds synthesized was confirmed by MALDI-TOF MS, HPLC-MS and HRMS. Purity was checked by RP-HPLC using a symmetry  $\text{C}_{18}$  column. Products showed purity of  $\geq 95$  (see Supporting Information).

### Parallel artificial membrane permeability assay (PAMPA)

The PAMPA<sup>[52]</sup> was used to determine the capacity of compounds to cross the BBB by passive diffusion. The effective permeability of the compounds was measured at an initial concentration of 200  $\mu\text{M}$ . The buffer solution was prepared from a concentrated one, commercialized by pION, and following the manufacturer's instructions. The pH was adjusted to 7.4 using a 0.5 M solution of NaOH. The compound of interest was dissolved in buffer solution or water (in the case of cargos alone, evaluated by HPLC-MS) and 1-propanol (20%, co-solvent) to the desired concentration (200  $\mu\text{M}$ ). The PAMPA sandwich was separated, and the donor well was filled with 200  $\mu\text{L}$  of the compound solution of interest. The acceptor plate was placed into the donor plate, ensuring that the underside of the membrane was in contact with buffer. The mixture of phospholipids (4  $\mu\text{L}$ , 20  $\text{mg mL}^{-1}$ ) in dodecane was added to the filter of each well, and buffer solution (200  $\mu\text{L}$ ) was added to each acceptor well. The plate was covered and incubated at room temperature under an atmosphere of saturated humidity for 4 h with orbital agitation at 100 rpm. After the 4 h, 150  $\mu\text{L}$  per well from the donor plate and 150  $\mu\text{L}$  per well from the acceptor plate were transferred to HPLC vials, and 100  $\mu\text{L}$  from each sample were injected onto an HPLC RP Symmetry  $\text{C}_{18}$  column (150 × 4.6 mm × 5  $\mu\text{m}$ , 100 Å, Waters). Transport was also confirmed by MALDI-TOF mass spectrometry to verify that the compound had kept its integrity. For PAMPA evaluated by HPLC-MS the same procedure was used, except that buffer solution was replaced by water and after the 4 h, 100  $\mu\text{L}$  per well from the donor plate and 100  $\mu\text{L}$  per well from the acceptor plate were transferred to HPLC-MS vials, and 10  $\mu\text{L}$  from each donor and 20  $\mu\text{L}$  from each acceptor were injected onto an HPLC-MS apparatus.

The phospholipid mixture used was a porcine polar brain lipid extract. Composition: phosphatidylcholine (PC) 12.6%, phosphatidylethanolamine (PE) 33.1%, phosphatidylserine (PS) 18.5%, phosphatidylinositol (PI) 4.1%, phosphatidic acid 0.8%, and 30.9% other compounds. The effective permeability after 4 h was calculated using Equation (1); the percentage of transport after was calculated using Equation (2):

$$P_e = \frac{-218.3}{t} \cdot \log \left[ 1 - \frac{2 \cdot C_A(t)}{C_D(t_0)} \right] \cdot 10^{-6} \text{ cm s}^{-1} \quad (1)$$

$$T\% = \frac{C_A(t)}{C_D(t_0)} \cdot 100 \quad (2)$$

in which  $t$  is time (h),  $C_A(t)$  is the compound concentration in the acceptor well at time  $t$ , and  $C_D(t_0)$  is the compound concentration in the donor well at 0 h. The membrane retention (%R) was calculated from the difference between the total starting amount and the amounts in donor and acceptor compartments at the end of the experiment ( $t = 4$  h).

### Immobilized artificial membrane chromatography (IAMC)

Retention times were determined using an IAMC column with phosphatidylcholine (PC), the major phospholipid in cell membranes, which was covalently immobilized (10 × 4.6 mm, 12  $\mu\text{m}$ , 300 Å, IAM.PC.DD2 column, Regis Technologies Inc.). The compounds were detected by UV absorption at 220 nm. The chromatograms were obtained by HPLC working isocratically with a mobile phase containing 10 mM phosphate buffer, 2.7 mM KCl, and 137 mM NaCl at pH 7.4 and 20% (v/v) MeCN. The retention times ( $t_R$ ) were transformed into capacity factors ( $k_{IAM}$ ) following Equation (3):

$$k_{IAM} = (t_R - t_0)/t_0 \quad (3)$$

in which  $t_R$  is the compound retention time (min), and  $t_0$  is the citric acid retention time (min), indicating the column dead time.

### HPLC-MS experiment for quantification of GABA and NIP

The HPLC-MS analysis was performed using a Waters 2795 Separation Module, operating in positive ion mode with a Waters 2487 Dual  $\lambda$  Absorbance detector. The HPLC column used was an RP Symmetry column (4.6 × 150 mm, 5  $\mu\text{m}$ ,  $\text{C}_{18}$ ). The samples were eluted at 1  $\text{mL min}^{-1}$  using different linear gradients of solvents A ( $\text{H}_2\text{O} + 0.1\%$  formic acid (v/v)) and B (MeCN + 0.07% formic acid (v/v)). The detection was performed at 220 nm. External standards at concentration of 0.2, 0.4, 1, 2, 4, 10, 20, 40, 80, 100, 120, 160, and 200  $\mu\text{M}$  were prepared by diluting the 1000  $\mu\text{M}$  stock solution with 20% 1-propanol in water. Prior to the experiments, the compounds were analyzed by HPLC-MS using scan mode to determine the retention time of each. For the experiments, single-ion monitoring (SIM) was used instead of a scan mode.

### Acknowledgements

This work was supported by MCI-FEDER (Bio2008-00799) and the Generalitat de Catalunya (XRB and 2009SGR-1005).

**Keywords:** blood-brain barrier • drug delivery • membranes • peptides

- [1] M. Malakoutikhah, M. Teixido, E. Giralt, *Angew. Chem. Int. Ed.* **2011**, *50*, 7998–8014; *Angew. Chem.* **2011**, *123*, 8148–8165.
- [2] W. M. Pardridge, *Brain Drug Targeting: The Future of Brain Drug Development*, Cambridge University Press, Cambridge, **2001**.
- [3] L. Malavolta, F. R. Cabral, *Neuropeptides* **2011**, *45*, 309–316.
- [4] W. M. Pardridge, *Drug Discovery Today* **2007**, *12*, 54–61.
- [5] W. M. Pardridge, *Pharm. Sci. Technol. Today* **1999**, *2*, 49–59.
- [6] L. L. Rubin, J. M. Staddon, *Annu. Rev. Neurosci.* **1999**, *22*, 11–28.

- [7] A. G. De Boer, P. J. Gaillard, *Annu. Rev. Pharmacol. Toxicol.* **2007**, *47*, 323–355.
- [8] Y. Chen, L. Liu, *Adv. Drug Delivery Rev.* **2012**, *64*, 640–665.
- [9] “Drug Delivery Strategies: BBB Shuttles”, R. Prades, M. Teixidó, E. Giralt in *Nanostructured Biomaterials for Overcoming Biological Barriers*, (Eds.: M. J. Alonso, N. S. Csaba), RSC Drug Discovery Series No. 22, **2012**.
- [10] W. M. Pardridge, *Curr. Opin. Pharmacol.* **2006**, *6*, 494–500.
- [11] R. Prades, S. Guerrero, E. Araya, C. Molina, E. Salas, E. Zurita, J. Selva, G. Egea, C. Lopez-Iglesias, M. Teixidó, M. J. Kogan, E. Giralt, *Biomaterials* **2012**, *33*, 7194–7205.
- [12] K. A. Witt, T. J. Gillespie, J. D. Huber, R. D. Egleton, T. P. Davis, *Peptides* **2001**, *22*, 2329–2343; R. D. Egleton, T. P. Davis, *Peptides* **2001**, *22*, 2329–2343.
- [13] M. Malakoutikhah, M. Teixido, E. Giralt, *J. Med. Chem.* **2008**, *51*, 4881–4889.
- [14] M. Malakoutikhah, R. Prades, M. Teixido, E. Giralt, *J. Med. Chem.* **2010**, *53*, 2354–2363.
- [15] M. Teixidó, E. Zurita, M. Malakoutikhah, T. Tarrago, E. Giralt, *J. Am. Chem. Soc.* **2007**, *129*, 11802–11813.
- [16] E. G. Chikhale, N.-Y. Ng, P. S. Burton, R. T. Borchardt, *Pharm. Res.* **1994**, *11*, 412–419.
- [17] E. M. Arnett, J. M. Gold, *J. Am. Chem. Soc.* **1982**, *104*, 636–639.
- [18] O. Cruciani, S. Borocci, R. Lamanna, G. Mancini, A. L. Segre, *Tetrahedron: Asymmetry* **2006**, *17*, 2731–2737.
- [19] C. Bombelli, S. Borocci, O. Cruciani, G. Mancini, D. Monti, A. L. Segre, A. Sorrenti, M. Venanzi, *Tetrahedron: Asymmetry* **2008**, *19*, 124–130.
- [20] C. Bombelli, S. Borocci, F. Lupi, G. Mancini, L. Mannina, A. L. Segre, S. Viel, *J. Am. Chem. Soc.* **2004**, *126*, 13354–13362.
- [21] S. C. D. N. Lopes, A. Fedorov, M. A. R. B. Castanho, *ChemMedChem* **2006**, *1*, 723–728.
- [22] K. A. Wit, C. A. Slate, R. D. Egleton, J. D. Huber, H. I. Yamamura, V. J. Hruby, T. P. Davis, *J. Neurochem.* **2000**, *75*, 424–435.
- [23] C. J. Bowerman, W. Liyanage, A. J. Federation, B. L. Nilsson, *Biomacromolecules* **2011**, *12*, 2735–2745.
- [24] B. M. Liederer, T. Fuchs, D. Vander Velde, T. J. Siahaan, R. T. Borchardt, *J. Med. Chem.* **2006**, *49*, 1261–1270.
- [25] A. Sorrenti, M. Diociaiuti, V. Corvaglia, P. Chistolini, G. Mancini, *Tetrahedron: Asymmetry* **2009**, *20*, 2737–2741.
- [26] F. H. McDowell, J. E. Lee, *West. J. Med.* **1970**, *113*, 44–46.
- [27] R. A. Hawkins, A. Mokashi, I. A. Simpson, *Exp. Neurol.* **2005**, *195*, 267–271.
- [28] A. Di Stefano, P. Sozio, L. S. Cerasa, *Molecules* **2008**, *13*, 46–68.
- [29] F. Pinnen, I. Cacciatore, C. Cornacchia, P. Sozio, A. Iannitelli, M. Costa, L. Pecci, C. Nasuti, F. Cantalamessa, A. Di Stefano, *J. Med. Chem.* **2007**, *50*, 2506–2515.
- [30] A. Di Stefano, M. Carafa, P. Sozio, F. Pinnena, D. Braghiroli, G. Orlan-  
do, G. Cannazzab, M. Ricciutell, C. Marianecid, E. Santucci, *J. Con-  
trolled Release* **2004**, *99*, 293–300.
- [31] G. Cannazza, A. Di Stefano, B. Mosciatti, D. Braghiroli, M. Baraldi, F. Pinnen, P. Sozio, C. Benatti, C. Parenti, *J. Pharm. Biomed. Anal.* **2005**, *36*, 1079–1084.
- [32] H. Sasaki, Y. Mori, J. Nakamura, J. Shibasaki, *J. Med. Chem.* **1991**, *34*, 628–633.
- [33] V. Carelli, F. Liberatore, L. Scipione, G. Giorgioni, A. Di Stefano, *Bioorg. Med. Chem. Lett.* **2003**, *13*, 3765–3769.
- [34] A. Kakee, H. Takanaga, T. Terasaki, M. Naito, T. Tsuruo, Y. Sugiyama, *J. Neurochem.* **2001**, *79*, 110–118.
- [35] Y. Zhang, G. Q. Liu, *Brain Res.* **1998**, *808*, 1–7.
- [36] V. E. Shashoua, J. N. Jacob, R. Ridge, A. Campbell, R. J. Baldessarini, *J. Med. Chem.* **1984**, *27*, 659–664.
- [37] H. H. Frey, W. Löscher, *Neuropharmacology* **1980**, *19*, 217–220.
- [38] L. Galzigna, L. Garbin, M. Bianchi, A.; Marzotto, *Arch. Int. Pharmacodyn. Ther.* **1978**, *235*, 73–85.
- [39] R. Barrett-Jolley, *Br. J. Pharmacol.* **2001**, *133*, 673–678.
- [40] E. F. Ali, W. E. Bondinell, P. A. Dandridge, J. S. Frazee, E. Garvey, G. R. Girard, C. Kaiser, T. W. Ku, J. J. Lafferty, G. I. Moonsammy, H. J. Oh, J. A. Rush, P. E. Setler, O. D. Stringer, J. W. Venslavsky, B. W. Volpe, L. M. Yunger, C. L. Zirkle, *J. Med. Chem.* **1985**, *28*, 653–660.
- [41] H. Fischer, M. Kansy, A. Avdeef, *Eur. J. Pharm. Sci.* **2007**, *31*, 32–42.
- [42] C. L. Gentry, R. D. Egleton, T. Gillespie, T. J. Abbruscato, H. B. Bechowski, V. J. Hruby, T. P. Davis, *Peptides* **1999**, *20*, 1229–1238.
- [43] S. J. Weber, D. L. Greene, S. D. Sharma, H. I. Yamamura, T. H. Kramer, T. F. Burks, V. J. Hruby, L. B. Hersh, T. P. Davis, *J. Pharmacol. Exp. Ther.* **1991**, *259*, 1109–1117.
- [44] H. M. Liu, X. F. Liu, J. L. Yao, C. L. Wang, Y. Yu, R. Wang, *J. Pharmacol. Exp. Ther.* **2006**, *319*, 308–316.
- [45] T. J. Abbruscato, S. A. Williams, A. Misicka, A. W. Lipkowski, V. J. Hruby, T. P. Davis, *J. Pharmacol. Exp. Ther.* **1996**, *276*, 1049–1057.
- [46] M. Teixidó, F. Albericio, E. Giralt, *J. Pept. Res.* **2005**, *65*, 153–166.
- [47] E. Biron, J. Chatterjee, O. Ovadia, D. Langenegger, J. Bruegggen, D. Hoyer, H. A. Schmid, R. Jelinek, C. Gilon, A. Hoffman, H. Kessler, *Angew. Chem. Int. Ed.* **2008**, *47*, 2595–2599; D. Langenegger, J. Bruegggen, D. Hoyer, H. A. Schmid, R. Jelinek, C. Gilon, A. Hoffman, H. Kessler, *Angew. Chem. Int. Ed.* **2008**, *47*, 2595–2599; *Angew. Chem.* **2008**, *120*, 2633–2637.
- [48] E. Kaiser, R. L. Colescott, C. D. Bossinger, P. I. Cook, *Anal. Biochem.* **1970**, *34*, 595–598.
- [49] A. Madder, N. Farcy, N. G. C. Hosten, H. De Muyck, P. J. De Clercq, J. Barry, A. P. Davis, *Eur. J. Org. Chem.* **1999**, 2787–2791.
- [50] P. Sieber, *Tetrahedron Lett.* **1987**, *28*, 2107–2110.
- [51] S. C. Miller, T. S. Scanlan, *J. Am. Chem. Soc.* **1997**, *119*, 2301–2302.
- [52] M. Kansy, F. Senner, K. Gubernator, *J. Med. Chem.* **1998**, *41*, 1007–1010.

Received: December 31, 2013

Published online on March 24, 2014